Experimental Cell Research 422 (2023) 113430

Contents lists available at ScienceDirect

Experimental Cell Research

journal homepage: www.elsevier.com/locate/yexcr

Research article

Spatial and temporal requirement of Mlp60A isoforms during muscle development and function in *Drosophila melanogaster*

Rohan Wishard [a,*], Mohan Jayaram [a,b], Saraf R Ramesh [b,c], Upendra Nongthomba [a,**]

[a] Department of Molecular Reproduction, Development and Genetics; Indian Institute of Science, Bengaluru, 560012, India
[b] Department of Studies in Zoology, University of Mysore, Manasgangotri, Mysuru, 570006, India
[c] Department of Life Sciences, Pooja Bhagvat Memorial Mahajana Education Center, K. R. S. Road, Mysuru, 570016, India

ARTICLE INFO

Keywords:
Muscle-LIM-Protein
Drosophila
Striated muscles
Isoform switching
Z-discs

ABSTRACT

Many myofibrillar proteins undergo isoform switching in a spatio-temporal manner during muscle development. The biological significance of the variants of several of these myofibrillar proteins remains elusive. One such myofibrillar protein, the Muscle LIM Protein (MLP), is a vital component of the Z-discs. In this paper, we show that one of the Drosophila MLP encoding genes, *Mlp60A*, gives rise to two isoforms: a short (279 bp, 10 kDa) and a long (1461 bp, 54 kDa) one. The short isoform is expressed throughout development, but the long isoform is adult-specific, being the dominant of the two isoforms in the indirect flight muscles (IFMs). A concomitant, muscle-specific knockdown of both isoforms leads to partial developmental lethality, with most of the surviving flies being flight defective. A global loss of both isoforms in a *Mlp60A*-null background also leads to developmental lethality, with muscle defects in the individuals that survive to the third instar larval stage. This lethality could be rescued partially by a muscle-specific overexpression of the short isoform. Genetic perturbation of only the long isoform, through a *P-element* insertion in the long isoform-specific coding sequence, leads to defective flight, in around 90% of the flies. This phenotype was completely rescued when the *P-element* insertion was precisely excised from the locus. Hence, our data show that the two *Mlp60A* isoforms are functionally specialized: the short isoform being essential for normal embryonic muscle development and the long isoform being necessary for normal adult flight muscle function.

1. Introduction

The postnatal development of vertebrate cardiac and skeletal muscles is marked by the switching of several sarcomeric contractile proteins from their foetal to the respective adult isoforms [1–7]. The cellular mechanisms by which these isoforms are regulated during striated muscle development have not been studied in detail. Also, the functional significance of this developmental isoform switching [8], and the redundancy/non-redundancy among the different isoforms of several of these sarcomeric contractile proteins awaits a detailed study [1,9–11]. The mixed population of fibre types in mammalian skeletal muscles makes it difficult to study the functions of the specific isoforms of sarcomeric proteins [4,12]. On the other hand, the Drosophila dorsal longitudinal muscles (DLMs), which are a type of indirect flight muscles (IFMs-a term which will be used to refer to DLMs henceforth, in order to maintain consistency with previous literature), offer a unique model system to study muscle development, due to their structural similarity with the vertebrate skeletal muscles [13,14], functional similarity with the vertebrate cardiac muscles [15,16], and a relatively uniform composition of only 'fibrillar' type fibres [16,17]. Moreover, the later stages of IFM development are similar to the postnatal development of the vertebrate striated muscles, since isoform switching of sarcomeric proteins occurs in both. In *Drosophila melanogaster*, several sarcomeric proteins, such as Myosin Heavy Chain (MHC), Actin, Troponin subunits, Tropomyosin, Myosin Light Chain (MLC), Kettin and Zormin, etc., are known to undergo isoform switching from their embryonic/larval to their respective adult isoforms, that are expressed either specifically in the IFMs, or in both the IFMs and the jump muscle, Tergal Depressor of Trochanter (TDT) [18–26]. Hence, IFM- or IFM-TDT-specific null mutants of different sarcomeric proteins have been isolated, which

* Corresponding author.
** Corresponding author.
E-mail addresses: rohanwishard@gmail.com, rohanwishard@alum.iisc.ac.in (R. Wishard), upendra.nongthomba@gmail.com, upendra@iisc.ac.in (U. Nongthomba).

https://doi.org/10.1016/j.yexcr.2022.113430
Received 23 July 2022; Received in revised form 18 November 2022; Accepted 19 November 2022
Available online 21 November 2022

facilitate the study of these stage and tissue specific isoforms [11,22,25,27–30].

In the present study, we show that the Muscle LIM Protein at 60A (Mlp60A) undergoes isoform switching during muscle development in *Drosophila melanogaster*. The vertebrate ortholog of Mlp60A is Cysteine and Glycine-rich Protein 3 (CSRP3). Cell culture studies have demonstrated that this protein can promote myogenic differentiation by associating with several muscle-specific transcription factors, such as MyoD, MRF4, and Myogenin [31,32]. Moreover, through knockout studies performed in a mouse model, this protein has been shown to be necessary for the development of cardiomyocyte cytoarchitecture. *CSRP3*$^{-/-}$ mice show dilated cardiomyopathy (DCM)- and hypertrophic cardiomyopathy (HCM)-like phenotypes [33,34]. *CSRP3* mutations have also been identified in human cardiomyopathy patients [35–38]. However, the precise role of MLP in muscle differentiation, and its requirement for skeletal muscle development have not been addressed. MLP is expressed in both developing and adult skeletal musculature in mice and zebrafish, but its deficiency in either of these model organisms produces only mild skeletal muscle phenotypes [33,39,40]. Hence, it is not understood whether this protein is dispensable for skeletal muscle development, or if some alternate isoform or paralog compensates for its deficiency. Interestingly, an alternate isoform of MLP, called the "MLP-b" isoform, was reported by Vafiadaki et al. [41]. This isoform was found to be upregulated in tissue samples from skeletal muscle disease patients and appeared to be a negative regulator of myogenesis [41]. However, the distinct spatio-temporal requirements of the two MLP isoforms in skeletal muscle development, and the precise role of the MLP-b isoform have not been addressed. Our results show that there is an exclusive functional specialization of the *Mlp60A* isoforms in *Drosophila melanogaster*, with one isoform being constitutive, and essential for embryonic muscle development, and the other being adult-specific, and necessary for normal flight.

2. Results

2.1. The Mlp60A locus in Drosophila melanogaster codes for two alternatively spliced isoforms, which localize to the sarcomere Z-discs and have distinct spatio-temporal expression profiles

In addition to the isoform reported earlier [42], the *Mlp60A* locus is predicted to produce a putative, second, alternatively spliced isoform (Fig. 1A, https://flybase.org/reports/FBgn0259209.html#gene_model

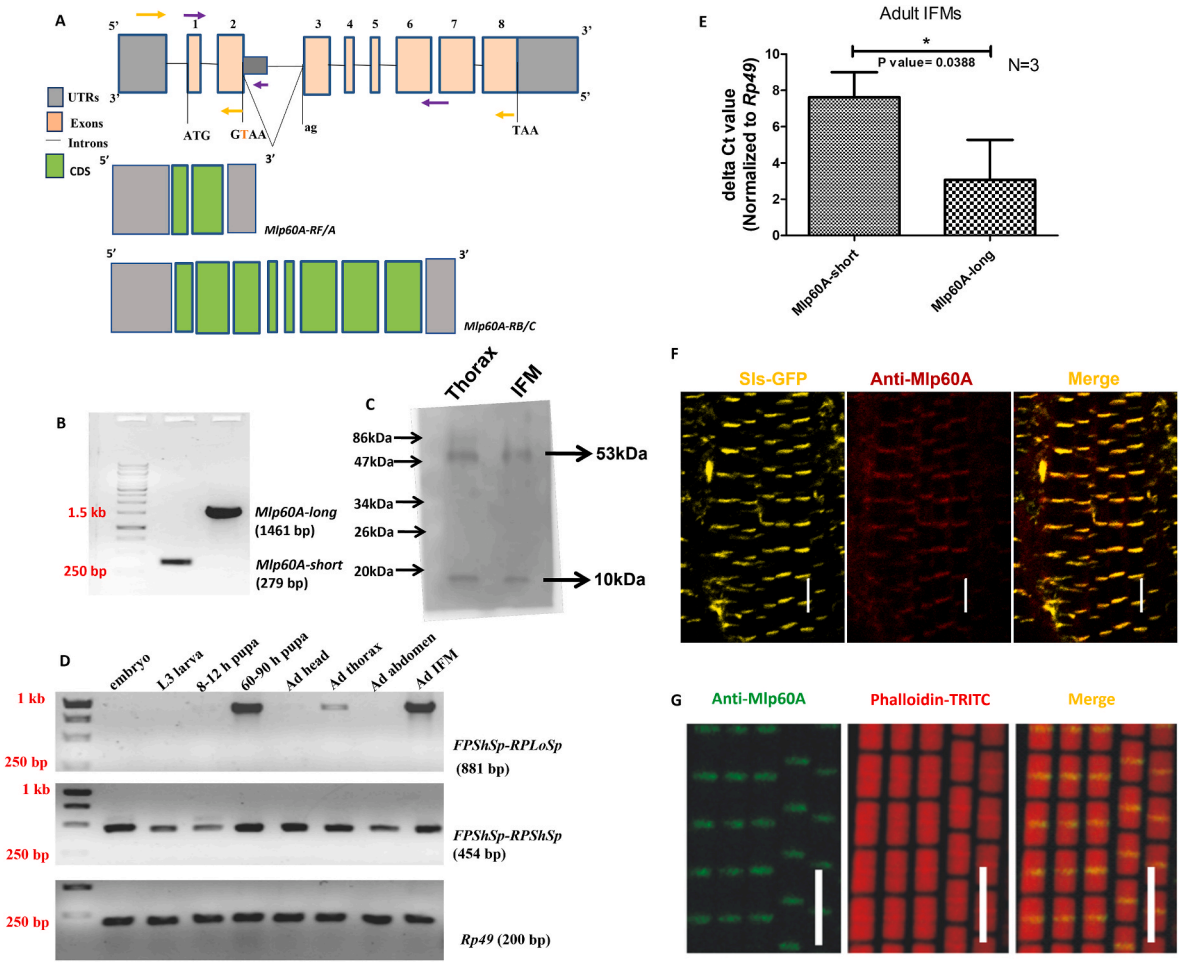

Fig. 1. Expression and developmental switching of alternatively spliced isoforms of Mlp60A. (A) Gene locus with the experimentally verified short isoform (*Mlp60A-RF/A*) and the bioinformatically predicted long isoform (*Mlp60A-RB/C*). The image is only schematic and not drawn to scale (B) 1% Agarose Gel showing the full-length *Mlp60A-short* and *Mlp60A-long* CDS, amplified from newly eclosed adult whole-body cDNA. These were amplified using primer combinations shown in yellow, in panel (A). A common forward primer: *FPShIsoCl*, was used with two different reverse primers: *RPShIsoCl,* for the short isoform and *RPLoIsoCl,* for the long isoform. (C) Western blot showing the two isoforms, detected with Mlp60A polyclonal antibody. (D) Expression profiling of *Mlp60A-short* and *Mlp60A-long* isoforms by qualitative RT-PCR. These were amplified using primer combinations shown in purple. A common forward primer (*FPShSp*) was used with a short isoform-specific (*RPShSp*) or long isoform-specific (*RPLoSp*) reverse primers. (E) Quantitative analysis of *Mlp60A-short* (using *Mlp60A_exon2_FP/RPShSp* primer pair) and *Mlp60A-long* (using *FPLoSp/RPLoSp* primer pair) isoforms by qRT-PCR, in adult DLMs. (F) Immunostaining of adult IFMs with anti-Mlp60 A polyclonal antibody (red), in Sls-GFP background. (G) Co-immunostaining of adult IFMs with anti-Mlp60A polyclonal antibodies and Phalloidin-TRITC. Scale bar-5 μm.

_products). We were able to experimentally validate the presence of transcripts encoding each of these isoforms in cDNA prepared from the whole body (Fig. 1B). The respective full-length amplicons of the transcripts were sequenced and analysed (Fig. S1A). The coding sequence (CDS) of the long transcript was submitted to GenBank (NCBI Accession No: MN990115). The sequence alignment revealed that the two transcripts share a common transcription start site and the first two exons of the locus. An alternative splicing event, as shown in Fig. S1B, leads to the expression of the long transcript. To check whether the long transcript is indeed translated, we generated polyclonal antibodies against the short isoform CDS (common to both isoforms) (Fig. S2). Through these, we were able to detect a bigger, 54 kDa isoform, corresponding to the long transcript (1461 bp) and a smaller, 10 kDa isoform, corresponding to the short transcript (279 bp) (Fig. 1B and C).

The expression pattern of the two isoforms was analysed across different developmental stages and in various tissues of the adult. As shown in Fig. 1D, the short isoform is expressed constitutively across all the developmental stages, and in different body segments of the adult. However, the long isoform expression commences only during the mid-pupal stages, following which it becomes restricted to the thorax, being very prominent in the IFMs. Since the IFMs express both the isoforms, their expression was analysed quantitatively in the adult IFMs. The expression of the long isoform was found to be significantly higher than that of the short isoform (Fig. 1E). Immunostaining of IFMs with Mlp60A polyclonal antibodies, either in a *sallimus (sls)-GFP* background (Fig. 1F) or co-stained with Phalloidin-TRITC (Fig. 1G), revealed that the Mlp60A antibodies localize specifically to the Z-discs of the sarcomeres with no signal detected from elsewhere in the cytoplasm. Hence this result shows that both the isoforms localize to the sarcomere Z-discs in the IFMs.

2.2. Concomitant muscle-specific knockdown of both the Mlp60A isoforms leads to pupal lethality and severe flight defect in the surviving progeny

To dissect the developmental and functional requirement of *Mlp60A*, we performed a conditional knockdown of both isoforms, beginning from late embryo/early L1 stage, using the *Gal4/UAS* system [43]. In order to restrict the knockdown to the muscles only, the *Dmef2-Gal4* line was used to drive two different RNAi lines for *Mlp60A* (both containing shRNA targeting the constitutive 2nd exon). Around 86% (Fig. 2A) and 94% (Fig. 2B) knockdown was achieved with RNAi lines 1 and 2, respectively. In both cases, a substantial number of pupae failed to eclose (Fig. 2C). However, the severity of this phenotype varied depending on the RNAi line used. Where, in case of RNAi line 2-mediated knockdown, 72% of the pupae showed lethality, in case of knockdown using RNAi line 1, the pupal lethality observed was 51%. The knockdown pupae which failed to eclose, did survive up to the late pupal stages (Fig. 2D). The knockdown individuals that did eclose were tested for their flight ability. 87% and 47% of the surviving flies were flight defective, when the knockdown was carried out with RNAi lines 1 and 2, respectively (Fig. 2E).

2.3. Mlp60A knockdown flies with defective flight show myofibrillar defects

In order to study the muscle phenotypes resulting from knockdown

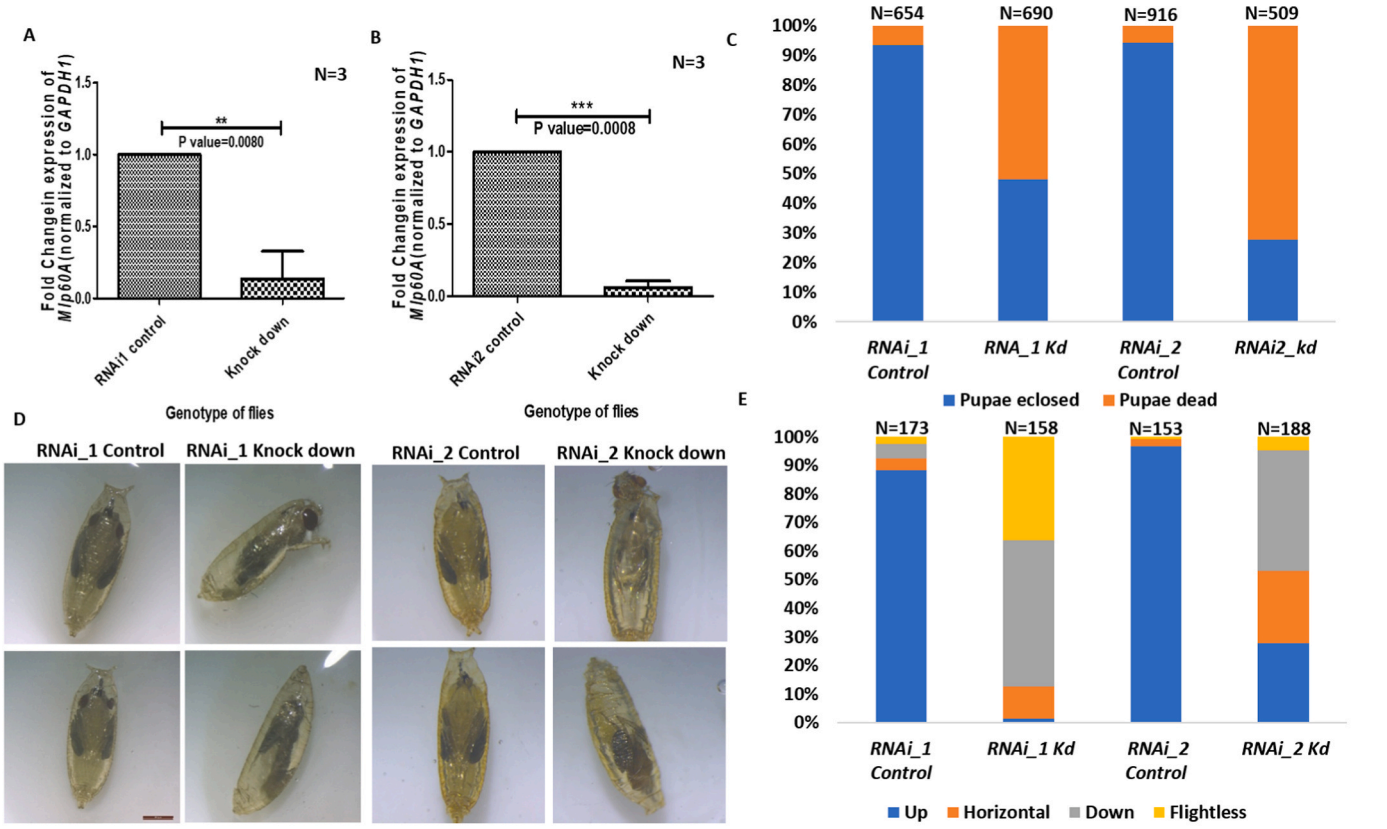

Fig. 2. Phenotypic effects of *Dmef2-Gal4* mediated knockdown of both *Mlp60A* isoforms. (A–B) Validation of knockdown with RNAi lines 1 (A) and 2 (B). (C) Assessment of pupal lethality in *Mlp60A* knockdown flies. Y-axis shows the percentage of pupae; X-axis shows the genotype of pupae. (D) Images of resulting dead pupae after *Mlp60A* knockdown. The scale bar = 200 nm. (E) Flight ability of 3–5 days old *Mlp60A* knockdown flies. Y-axis shows the percentage of flies; X-axis shows the genotype of flies.

of both Mlp60A isoforms, the flight-defective *Dmef2-Gal4::UAS-Mlp60A-RNAi_1* (knockdown) flies were processed for visualizing the IFM patterning and fascicular structure, using polarized optics. The IFMs of the knockdown flies did not differ significantly from the control IFMs in either their pattern (Fig. S3A) or fascicular dimensions (Figs. S3B–C). Next, flies of the same genotype were processed for observing the IFM myofibrillar structure using confocal microscopy. While the IFMs of the knockdown flies mostly showed myofibrils which were comparable in appearance to those of the control, they did contain a few frayed myofibrils (represented by white arrows) (Fig. 3A). Also, the knockdown IFMs had a reduced resting sarcomere length as compared to the control ones (see a magnified view of the longitudinal sections in Fig. 3A, quantification shown in Fig. 3D). The cross-sections of *Mlp60A*-knockdown IFMs revealed several actin-rich aggregates, which, although mostly concentrated along the IFM fascicular membrane (represented by white arrows in Fig. 3B), were also seen on the membranes of the internal myofibres (represented by black arrows in Fig. 3B). Most importantly, this phenotype was completely penetrant in the *Mlp60A*-knockdown flies and was not observed in any of their control counterparts. This phenotype suggests that *Mlp60A* could be involved in the regulation of thin filament assembly and actin dynamics. There was no significant difference in the fascicular cross-sectional area between the control and knockdown flies (Fig. 3C).

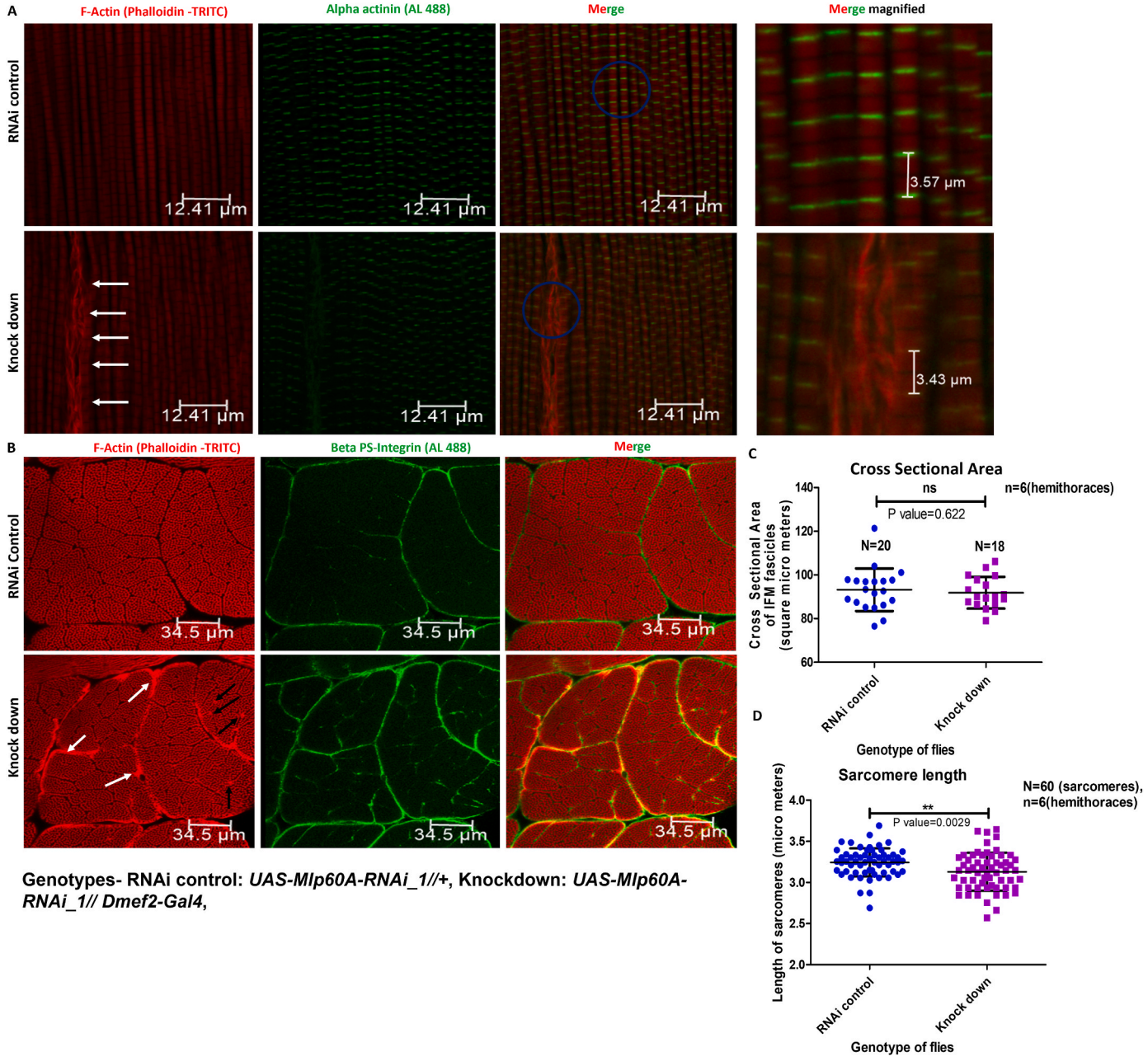

Genotypes- RNAi control: *UAS-Mlp60A-RNAi_1//+*, Knockdown: *UAS-Mlp60A-RNAi_1// Dmef2-Gal4*,

Fig. 3. IFM myofibrillar defects in *Mlp60A* knockdown flies. (A) Longitudinal sections of IFMs from 3 to 5 days old *Mlp60A* knockdown flies and the corresponding control flies were stained for F-actin filaments (red) and α-actinin (green). The frayed myofibrils seen in *Mlp60A* knockdown flies are marked with white arrows. (B) Transverse (Cross) sections of IFMs from 3 to 5 days old *Mlp60A* knockdown flies, stained for F-actin filaments (red) and β-PS Integrin (green). Actin-rich aggregates in the knockdown IFMs, deposited on the fascicular membrane and the membrane of internal myofibres, are marked with white and black arrows, respectively. (C) Quantification of the cross-sectional area of IFM fascicles. (D) Quantification of sarcomere length of IFM myofibrils. Genotypes- RNAi_1 Control: *UAS-Mlp60A-RNAi_1(III)*, RNAi_1 Knockdown: *Dmef2-Gal4(III)::UAS- Mlp60A-RNAi_1(III)*.

2.4. Isolation and characterization of Mlp60A mutant alleles by P-element hop out mutagenesis

To study the respective functions of the two isoforms, we performed a *P-element* hop-out mutagenesis screen to isolate null and isoform-specific mutant alleles of *Mlp60A*. For this purpose, a Bloomington fly line, BS#27970, carrying a *P-element* (*P{EP}*) insertion in the *Mlp60A* long isoform coding sequence, was obtained. The position and orientation of the *P{EP}* insertion were confirmed by PCR (Fig. S4). Flies having the *P-element* insertion were crossed with flies containing a gene coding for the delta 2–3 transposase to obtain the hop-out progeny in the next generation (described in Materials and Methods). We screened for only recessive alleles, which in homozygous condition, caused developmental lethality and/or weak or defective flight in the surviving flies or both (Table 1), consistent with the phenotypes observed in the knock-down experiments.

In order to characterize the mutant alleles, we began by selecting a suitable control allele, which would be one resulting from the precise excision of the inserted *P-element* and the 8 bp target site duplication [44], which a *P-element* insertion is known to cause, thus restoring the sequence at the insertion site to the wild type sequence. For this purpose, several candidate alleles which did not give rise to any developmental lethality, when homozygous, were tested for their flight ability (Fig. S5A). *UR 2.2.10* homozygous flies flew almost as good as the wild-type reference (Fig. S5A). PCR amplification and sequencing of the region flanking the insertion site, from these flies (Fig. S5B), confirmed that this particular allele was indeed a precise excision allele. Henceforth, the allele *UR 2.2.10* was renamed as the 'PEC' (precise excision control) allele.

Having selected a suitable control allele, we proceeded to characterize the respective genomic lesions in each of the homozygous lethal alleles, by performing PCR using overlapping primer pairs covering the insertion site (Fig. S6A). Fig. 4 is a schematic representation of the different mutant alleles described in this report. The lethal allele *UR 2.9.17*, was found to lack the genomic region spanning the first two exons of the *Mlp60A* region, the 5′-UTR, the intergenic region between *Mlp60A* and its upstream gene, *CG3209,* as well as the last two exons of *CG3209* (Figs. S6B–D). The allele *UR 2.10.7* was found to harbour a remnant of the *P-element* insertion at the original insertion site (Fig. S6B, lane *UR 2.10.7*). The transcripts produced by each of these alleles and the phenotypes of the corresponding homozygous mutants have been described further. The allele *UR 2.4.1* was found to lack a portion of the intron between exons 2 and 3 of the *Mlp60A* region (Fig. S6B, lane *UR 2.4.1*). This allele was found to complement both, the $Mlp60A^{null}$ allele (characterized in detail in this report) and a genomic deficiency covering the *Mlp60A* region, with regards to survival and flight ability (Fig. S13). Hence, this allele was not studied further.

2.5. Loss of Mlp60A leads to severe developmental lethality and larval body wall muscle defects

UR 2.9.17 homozygous L3 larvae were tested for the presence of any *Mlp60A* transcript, by RT-PCR. In these larvae, the *Mlp60A* short transcript (the only isoform detected at this stage in the wild-type flies, Fig. 1D) could not be detected, even when the reaction was carried up to saturation (Fig. 5A). Henceforth, the *UR 2.9.17* allele will be referred to as the $Mlp60A^{null}$ allele. To determine the effective lethal stage of the homozygous $Mlp60A^{null}$ individuals, we performed a lethality test, beginning from the L1 stage. Most of the null individuals perished during the larval stage itself (Fig. 5B). As a readout for muscle defects, $Mlp60A^{null}$ L3 larvae were assayed for their crawling ability. These larvae crawled smaller distances compared to the homozygous *PEC* larvae, when tested for the same duration of time (Fig. 5C). This phenotype was found to be statistically significant (Fig. 5D). Some of these larvae were then dissected to observe the body wall muscles. As shown in Fig. 5E, the $Mlp60A^{null}$ homozygous larvae showed defective body wall muscles, showing significant thinning compared to the control larvae (Fig. 5F). While most of the null larvae had degenerated or malformed muscles, few showed a more severe 'missing muscles' phenotype. Fig. 5E shows two representative images of the larval body wall muscles from each of the genotypes tested (defective/degenerated or absent muscles have been marked with white arrows).

To confirm that it is indeed the abrogation of *Mlp60A* expression which is responsible for the phenotypes observed in the $Mlp60A^{null}$ homozygous larvae, we performed a complementation test between the $Mlp60A^{null}$ allele and a genomic deficiency covering the *Mlp60A* region: *Df(2R)BSC356* (verified in Fig. S7B). The majority of the $Mlp60A^{null}$*//Df(2R)BSC356* progeny also failed to complete development (Fig. S7A). The L3 *trans*-heterozygotes were found to have severely compromised crawling ability (Figs. S7C–D), and also showed body wall muscle defects reminiscent of those observed in the $Mlp60A^{null}$ homozygotes (compare Figs. S7E and F with Fig. 5E and F, respectively).

2.6. Muscle-specific transgenic expression of Mlp60A short isoform partially rescues the developmental lethality associated with the $Mlp60A^{null}$ mutation

In order to further test whether the developmental lethality of $Mlp60A^{null}$ mutants is specifically due to the absence of the *Mlp60A-short* isoform, we sought to perform a rescue experiment by expressing only the *Mlp60A-short* isoform in the $Mlp60A^{null}$ background. For this purpose, we generated a transgenic fly line in which *UAS* regulatory sequences drive the expression of the full-length *Mlp60A-short* isoform (see Materials and Methods, and Figs. S8–9). *UH3-Gal4*, which has mild ubiquitous expression from 0 h after puparium formation (APF) to 42–46 h APF, following which it becomes restricted to the IFMs [45], was used to achieve an appreciable overexpression (Fig. S10A). The overexpression, by itself alone, did not elicit any phenotype (Fig. S10B). Ectopic expression of the short isoform driven by *UH3-Gal4* showed partial rescue of the developmental lethality observed in the $Mlp60A^{null}$ mutants (Fig. 6A). The expression level of the *Mlp60A-short* transcript achieved by the *Gal4/UAS* system was lesser than its endogenous expression levels in the wild type (Fig. 6B and C). The rescued flies were also tested for their flight ability. Around 40% of the rescued flies were flight defective, whereas another 20% showed reduced flight ability, being horizontally flighted (Fig. 6D). This flight profile was drastically different from that of the corresponding positive control flies, 80% of which were Up flighted. These results show that the short isoform alone cannot compensate for the loss of the long isoform, in the adults.

2.7. Loss of Mlp60A leads to down-regulation of several thin filament proteins

We hypothesised that loss of *Mlp60A* could lead to down-regulation of other thin and/or thick filament proteins. We based this hypothesis on three lines of reasoning. First, loss of a specific muscle contractile protein is known to result in coordinated transcriptional down-regulation of several other contractile proteins [24,30,46,47]. Second, the mammalian ortholog of *Mlp60A*, *CSRP3*, is necessary for muscle differentiation [31,32]. Third, our results revealed that $Mlp60A^{null}$ larvae possess thinner muscle fibres (Fig. 5E and F). Hence, to test our hypothesis, we

Table 1
Screening statistics for *Mlp60A_3*rd *exon_P{EP}* hop out screen.

Total No. Of Chromosomes Screened	3000
Total No. Of hop out chromosomes collected	77 (frequency of hopping out=2.56%)
Homozygous lethal Chromosomes	03
Of these, Homozygous lethal with flight defective survivors	01
Probable frequency of imprecise excision	0.1%

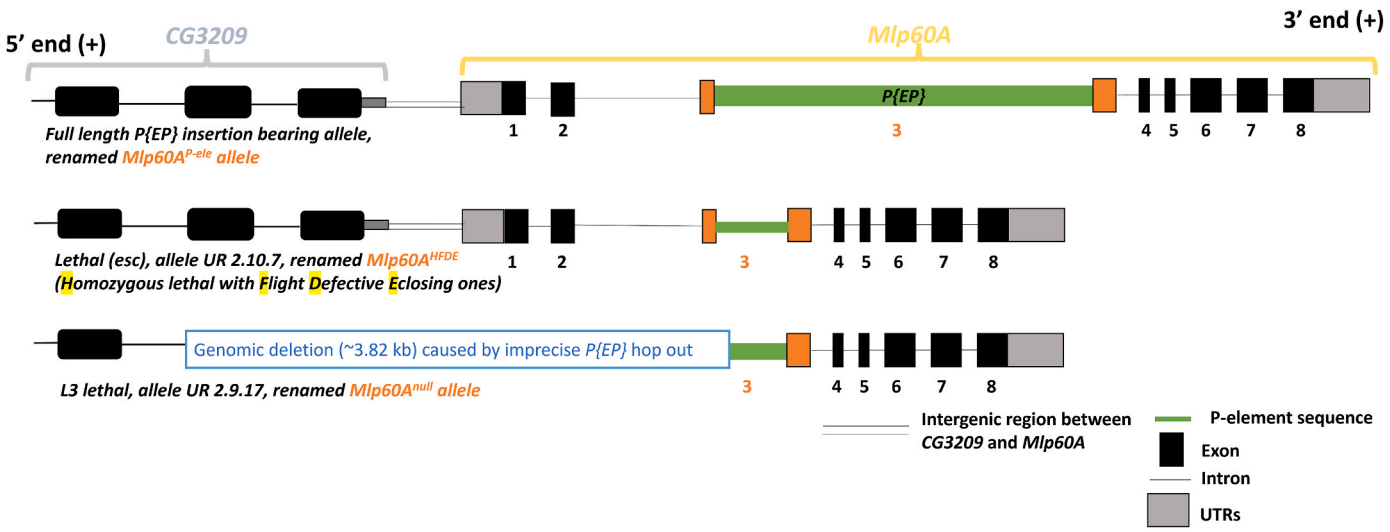

Fig. 4. Schematic representation of the different mutant alleles generated and described in this study. The diagram shows the *Mlp60A* locus and a part of the preceding locus-*CG3209*. The exons have been numbered 1–8 and shown as black boxes, except the 3rd exon, whose sequence has been shown by orange boxes. The *Mlp60A*$^{P\text{-}ele}$ allele is a *Mlp60A-long* specific mutant allele, which carries a full-length *P{EP}* insertion in the *Mlp60A-long* specific 3rd exon (hence, shown split-up). This allele served as the starting allele to generate the *Mlp60A*^{HFDE} allele, another *Mlp60A-long* specific allele and the *Mlp60A*^{null} allele. This was achieved by mobilizing the *P element* insert (*P{EP}*) from the *Mlp60A*$^{P\text{-}ele}$ allele and then screening for imprecise hop-out alleles. See text for details and see Fig. S6 for genomic characterization of these alleles.

analysed the expression of transcripts encoding six major muscle contractile proteins, in *Mlp60A*^{null} mutant larvae. Interestingly, expression of the majority of thin filament protein encoding transcripts was found to be significantly down-regulated in *Mlp60A*^{null} homozygotes as compared to the control (Fig. 7). The expression *of Myosin heavy chain (Mhc)*, the only tested gene encoding a thick filament protein, did not vary significantly between the test and the control larvae.

2.8. *Mlp60A-long isoform-specific mutants show drastically compromised flight ability*

To determine the function of the *Mlp60A-long* isoform, we characterized both the full-length *P-element* insertion allele in the Bloomington line *BS#27970* (renamed *Mlp60A*$^{P\text{-}ele}$, to denote the presence of a full-length *P{EP}* insertion, and referred to in data panels as, '*P-ele*') and the imprecise hop out allele *UR 2.10.7* (Fig. S6, renamed *Mlp60A*^{HFDE}, short for 'Homozygous Flight Defective Eclosing ones, and referred to in data panels as '*HFDE*'). We confirmed the insertion of the ~8 kb full-length *P{EP}* element within the 3rd exon of the *Mlp60A* locus, in *Mlp60A*$^{P\text{-}ele}$ homozygous flies (Fig. S4). A PCR, performed using genomic DNA, isolated from *Mlp60A*^{HFDE} homozygous individuals, as the template, and primers covering the insertion site, produced an amplicon of greater size (~1.3 kb higher) than those obtained from both the wild type and the *PEC* homozygous flies (Fig. 8A). The proportion of homozygous *Mlp60A*^{HFDE} flies, in the *Mlp60A*^{HFDE}*//CyO-GFP* balanced stocks, was found to be significantly lesser than that expected according to the Mendelian ratio for a monohybrid cross (which is shown by the positive control) (Fig. 8C). However, when complementation tests were performed between the different alleles, flies with both *Mlp60A*^{HFDE}*//Mlp60A*^{null} and *Mlp60A*^{HFDE}*//Df* genotypes were obtained as per the expected Mendelian ratio (as shown by the positive control) (Fig. 8C). Thus, the *Mlp60A*^{HFDE} allele can complement both the *Mlp60A*^{null} allele as well as a genomic deficiency covering the *Mlp60A* region, with regards to developmental lethality. This shows that the developmental lethality observed upon *Mlp60A*^{HFDE} homozygosity cannot be attributed specifically to this allele. This lethality could, probably, result from the homozygosity of a second site mutation on the *Mlp60A*^{HFDE} bearing chromosome, which could have been generated during the hop out. The *Mlp60A*$^{P\text{-}ele}$ allele itself is known to be non-lethal, as stable *Mlp60A*$^{P\text{-}ele}$ homozygous fly stocks have been maintained not only in our laboratory, but also at the Bloomington Drosophila Stock Center (BS#27970).

Next, the *Mlp60A*$^{P\text{-}ele}$ homozygous flies and *Mlp60A*^{HFDE} homozygous flies were tested for their flight ability (Fig. 8D). Around 37% and 48% of the *Mlp60A*$^{P\text{-}ele}$ homozygous flies were found to be flight-defective and weak-flighted, respectively (Fig. 8D). The flight defect was completely rescued in the *PEC* homozygous flies, whose flight ability was comparable to that of the wild type flies (Fig. 8D, compare 2nd, 3rd and 1st bars). On the other hand, as many as ~95% of the *Mlp60A*^{HFDE} homozygous flies were flight defective, and the remaining 5% weak flighted (Fig. 8D).

To determine how the presence of the transposon insertion within these two long isoform mutant alleles affects the transcription from the locus, we performed RT-PCR with primers covering the splice site and the insertion site. With cDNA templates prepared from the *Mlp60A*$^{P\text{-}ele}$ homozygous flies and *Mlp60A*^{HFDE} homozygous flies, the amplicons obtained appeared slightly truncated as compared to the ones obtained from the wild-type and *PEC* homozygous flies (Fig. 8B). As expected, the amplicons corresponding to the short isoform transcript, obtained from the *Mlp60A*$^{P\text{-}ele}$ homozygous flies and *Mlp60A*^{HFDE} homozygous flies, were identical in size, to those obtained from the wild type and *PEC* homozygotes (Fig. 8B). The sequences of amplicons corresponding to the long isoform transcripts, encoded by the *Mlp60A*$^{P\text{-}ele}$ and *Mlp60A*^{HFDE} alleles respectively, when aligned with each other (Fig. S11), were found to be completely identical (GenBank Accession no: MN990116). These transcript sequences were then aligned with the sequence of the corresponding wild type transcript, to determine the extent of the truncation (seen in Fig. 8B). Fig. S12 depicts the analysis of the region flanking the original insertion site. As shown by Fig. S12 A, both of the transcripts contain a unique stretch of 17 bases, which is not represented in the wild-type transcript sequence (shown by purple ovals), and both are devoid of a stretch of nucleotides, which is present in the wild-type transcript (shown by orange rectangles). Further analysis (Fig. S12B) revealed that these transcripts resulted from an alternative splicing event, in which the usual splice acceptor is bypassed and a novel splice acceptor, preceding the 4th exon is selected instead. However, the normal splice donor persists, resulting in the splicing out of the 3rd exon and the inclusion of a sequence of 17 bases (1726th −1742nd base) from intron 3–4, in the mature spliced transcript, thus ensuring that the

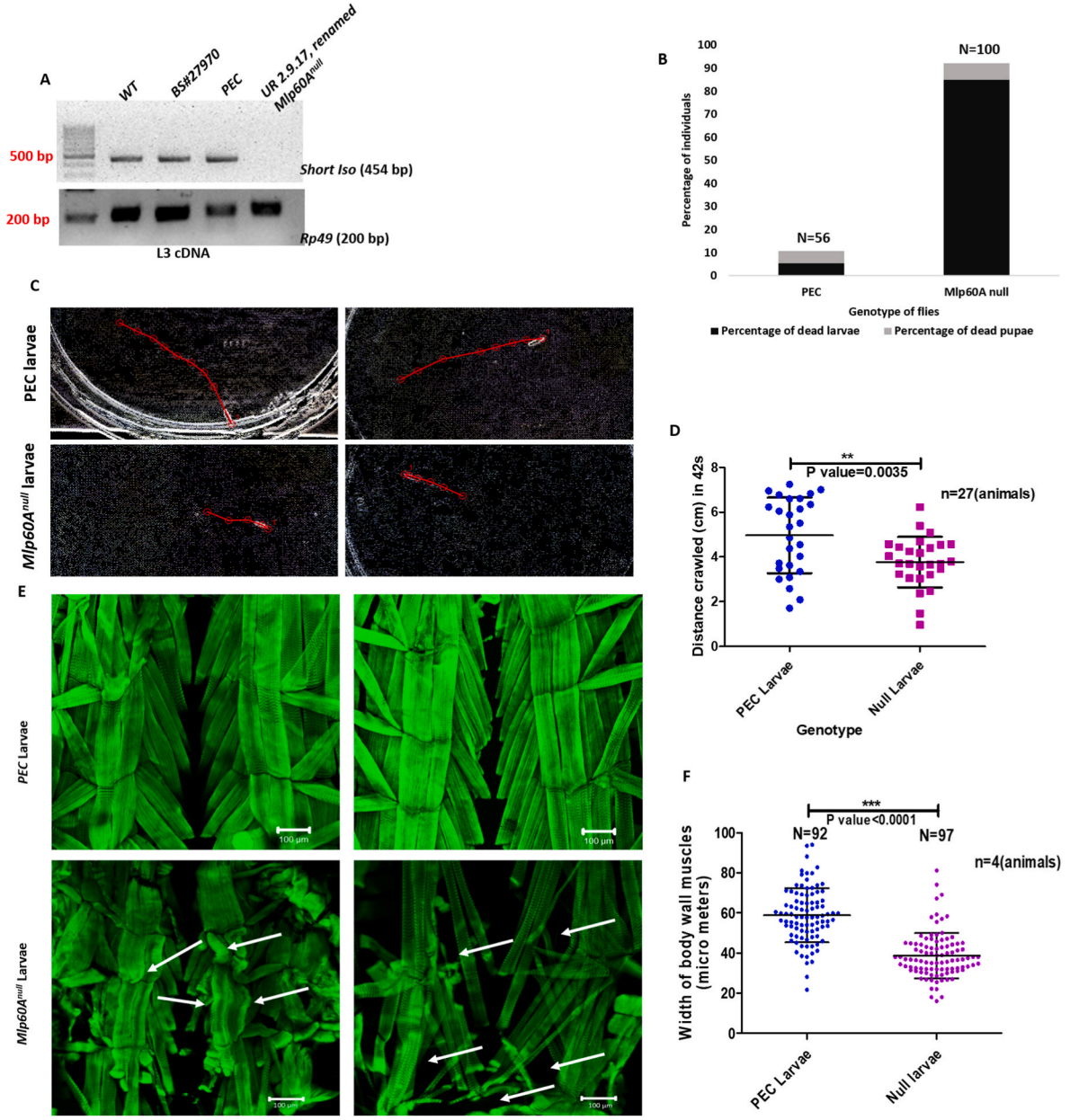

Fig. 5. Phenotype of *Mlp60A*^{null} homozygous larvae. (A) Analysis of *Mlp60A-short* expression in *UR 2.9.17* homozygous, BS27970# and *PEC* homozygous L3 larvae, along with w^{1118} larvae as control. Following this, the allele *UR 2.9.17* was renamed as *Mlp60A*^{null} allele. (B) Assessment of developmental lethality of *Mlp60A*^{null} homozygous larvae, beginning from the L1 developmental stage. (C) Two representative traces, each for *Mlp60A*^{null} homozygous and *PEC* homozygous L3 larvae, on a 1% agar plate. (D) Quantification of crawling ability of *Mlp60A*^{null} homozygous L3 larvae. (E) Body wall muscle defects visible in *Mlp60A*^{null} L3 larvae. The malformed muscles and regions of missing muscles have been marked with white arrows. (F) Quantification of the width of body wall muscles in *Mlp60A*^{null} homozygous L3 larvae.

insertion in the 3rd exon does not lead to a complete disruption of the reading frame (Fig. S12B). The translated protein sequences from both the truncated transcript sequences were aligned with the sequence of the wild type Mlp60A-long protein (Fig. 8E). This alignment showed that the aberrant splicing in both the *P-element* insertion alleles results in the removal of a total of 34 amino acid residues (93rd to 126th residues), encoded by the 3rd exon. Of these, 21 residues (106th to 126th residues) belong to the second LIM domain of the longer isoform. Also, 6 unique residues (WCSLSQ), encoded by the extra nucleotides in the mature transcript from both the *P-element* insertion alleles, are included in the protein sequence. Hence the *P-element* insertion in both these alleles leads to the expression of a mutant *Mlp60A-long* isoform, which has a truncated and modified second LIM domain. Overall, the flight phenotype of the *Mlp60A*$^{P\text{-}ele}$ homozygous flies and its subsequent rescue in the homozygous *PEC* flies suggests that the wild type Mlp60A-long isoform with all intact LIM domains is essential for normal flight.

3. Discussion

3.1. The short isoform of Mlp60A is necessary for the normal development of larval muscles

The Muscle LIM protein has long been regarded as a differentiation factor, which promotes the differentiation of myoblasts into myocytes in culture [31,32,49]. However, its role during the development of embryonic muscles, which are the first differentiated muscle structures *in*

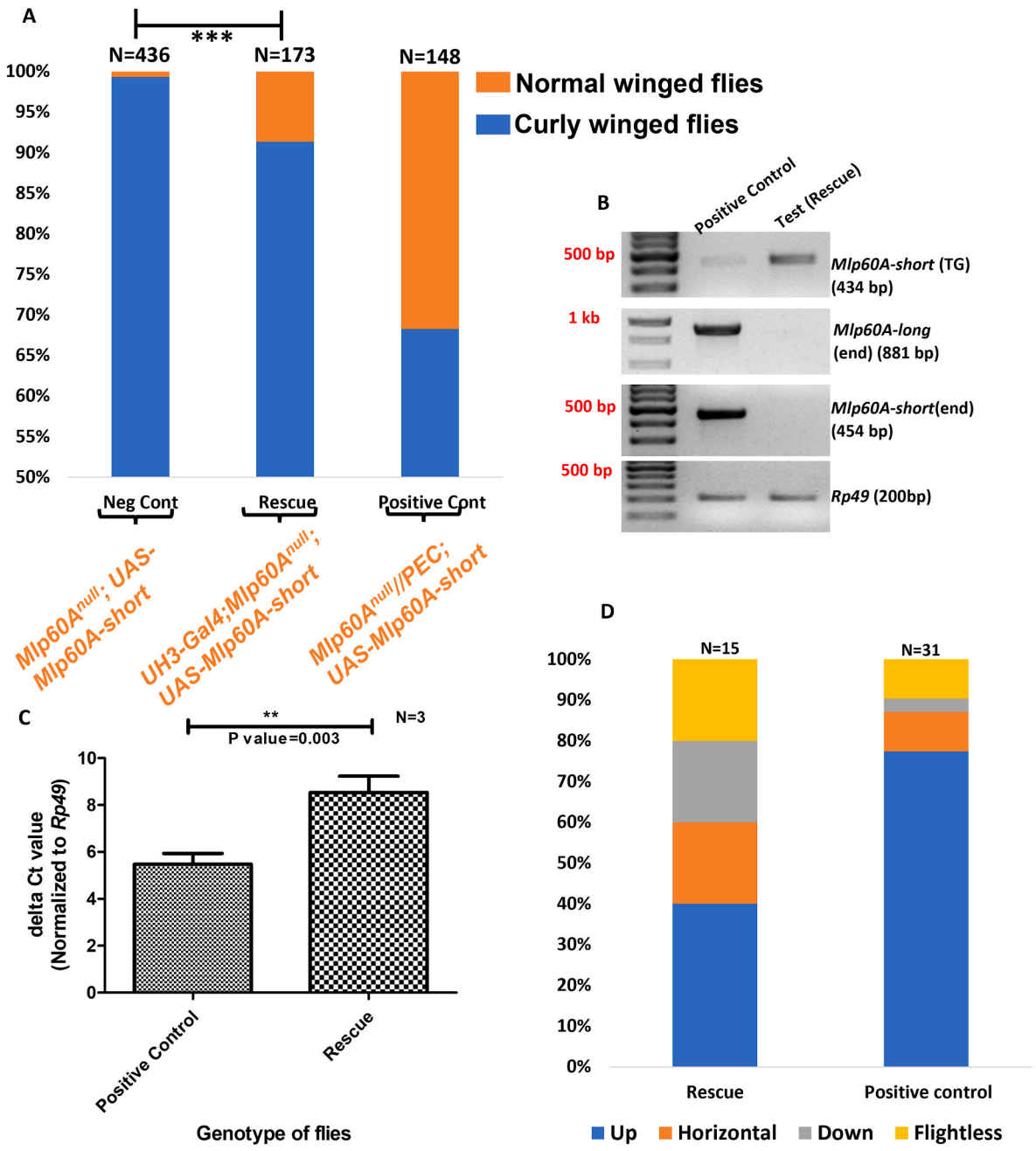

Fig. 6. Rescue of Mlp60A null individuals by transgenic overexpression of *Mlp60A-short* isoform. (A) Shows the percentage of normal and curly winged flies (Y-axis) obtained in the test (rescue), negative and positive control cross sets (X-axis). For the difference in the percentage of normal-winged flies in the negative control and test sets, P value < 0.0001, Chi-Square Value (CSV) $= 64.646$, df $= 1$. A complete rescue would have yielded a percentage of normal-winged flies, comparable to that in the positive control. Genotypes of normal-winged flies in each set have been specified in orange font. For detailed methodology, see Materials and Methods. (B) Shows the qualitative analysis of endogenous *Mlp60A-short* (labelled as 'end'), *Mlp60A-long* and transgenic *Mlp60A-short* (labelled as 'TG') isoforms from positive control and rescued fly-thoraces. The distinction between the endogenous and transgenic *Mlp60A-short* transcripts was made by using a common forward primer-FPShSp (no. 11 in Table S1), with different reverse primers, either RPShSp (no. 12 in Table S1) for the endogenous transcript, or Fab1 (no 49 in Table S1) for the transgenic transcript. (C) Shows the quantitative estimation of the levels of endogenous *Mlp60A-short* and transgenic *Mlp60A-short* from the positive control and rescued flies, respectively. (D) Shows the flight ability of the rescued and positive control flies (3–5 days old). Y-axis shows the percentage of flies; X-axis shows the genotype of flies. Genotypes- Negative control: *Mlp60A^{null}; UAS-Mlp60A-short*; Positive control: *PEC//Mlp60A^{null}; UAS-Mlp60A-short*; Rescue (test): *UH3-Gal4; Mlp60A^{null}; UAS-Mlp60A-short*.

vivo [50], has not been studied in detail. Our results show that this protein is necessary for the development of the larval body wall muscles of *Drosophila melanogaster*, which originate during the embryonic development [51]. Since the locomotion and body wall muscle defects in the *Mlp60A^{null}* mutants were seen at the L3 stage and not at the earlier stages (data not shown), it is likely that the *Mlp60A-short* isoform could be required for the maintenance of the larval body wall muscles. It is known that the body wall muscles, after initial development in the embryo, increase drastically in size (~25–40-fold increase in area) by hypertrophic growth, as the development proceeds from the L1 to L3 stage [52]. The myofibrillar-contractile proteins form a major portion of the dry weight of muscles, and an increase in muscle size is due to an increase in the contractile protein content [53]. We found that the expression of transcripts coding for a few major sarcomeric structural

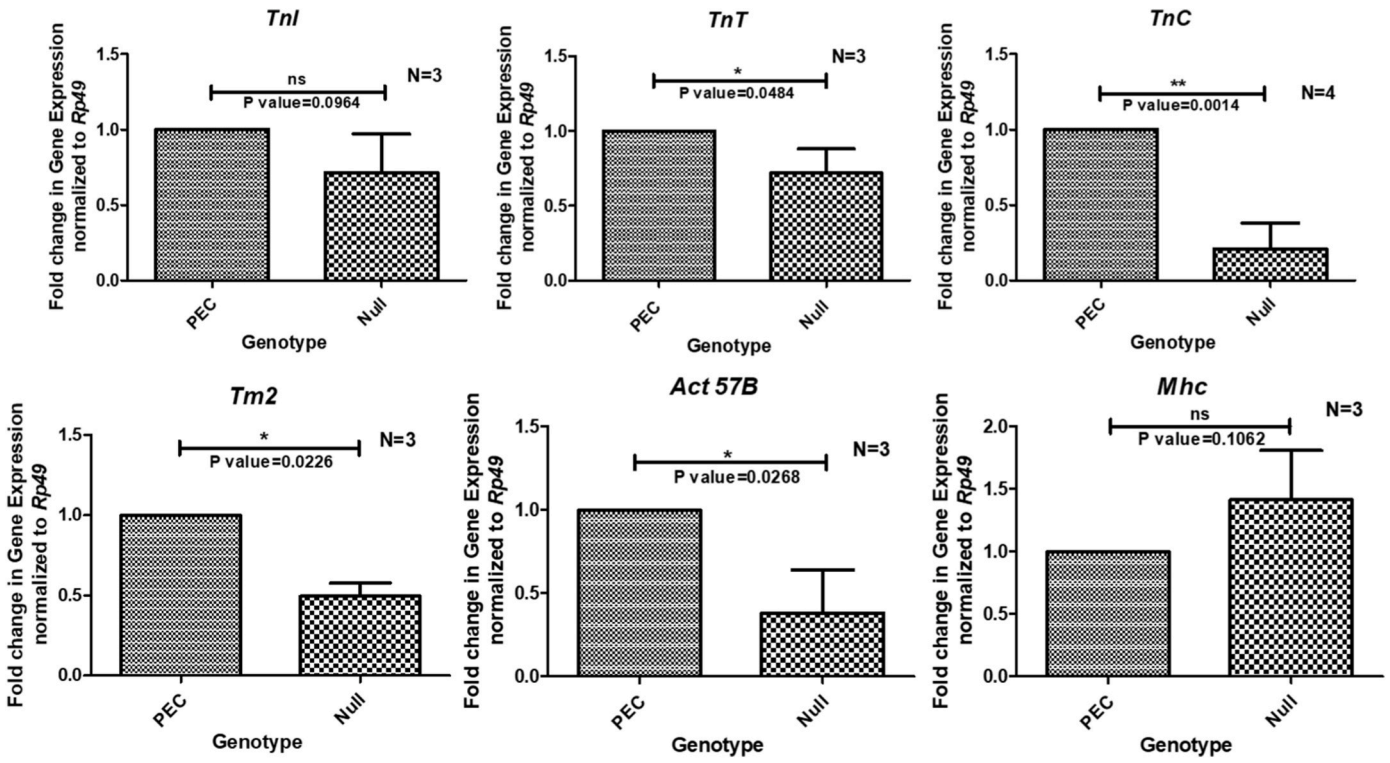

Fig. 7. Relative expression (measured by qRT-PCR, using the delta (delta Ct) method), of some major sarcomere protein-coding genes in *Mlp60A*^{null} L3 larvae. Transcript levels of most of the thin filament proteins were downregulated.

proteins, particularly thin filament proteins, was significantly reduced in *Mlp60A*^{null} homozygotes (Fig. 7). Therefore, it is likely that the complete absence of Mlp60A, a thin filament protein [49,54,55], and the resultant reduction in the transcripts of other major thin filament proteins, such as Actin (57B), Troponin I, Troponin T, Troponin C and Tropomyosin 2, leads to the reduction of muscle thickness and muscle loss, seen in the *Mlp60A*^{null} mutants. However, Myosin heavy chain expression was not affected in the *Mlp60A*^{null} mutants, unlike what was reported by Rashid et al. upon depletion of the MLP *in vitro* [56]. It is also important to note here that the phenotype shown by the *Mlp60A*^{null} homozygotes cannot result from the partial *CG3209* disruption, which the *Mlp60A*^{null} allele bears, since the *CG3209* loss of function mutants, characterized by Yan et al., did not show any post-L1 lethality or L3 stage locomotion defects [57]. Therefore, it can be concluded that the Mlp60A-short isoform is essential for the development of the larval body wall muscles. On the other hand, the other MLP ortholog-Mlp84B does not appear to play any role in the development of the larval body wall muscles since the *Mlp84B*^{null} mutants do not show any phenotype until the onset of pupal development [58].

3.2. *The two isoforms of Mlp60A are functionally specialized*

The expression profile of *Mlp60A* isoforms (Fig. 1C- E) mimics that of several other sarcomeric proteins, which have IFM or IFM-TDT-specific isoforms [22,25,27–30]. Such an expression profile suggests the presence of functional specialization among these isoforms [11,24,30,59,60]. Several studies conducted previously have shed light on the functional non-redundancy of the different isoforms of myofibrillar proteins, in Drosophila. Several dominant flightless, point mutants of *Act88F*, which codes for the IFM-specific actin isoform, Act88F, have been isolated [61,62]. Further, it has been shown that Act88F can functionally compensate for the loss of Act79B, the TDT-specific isoform, but the converse is not true [63]. The IFM-TDT specific TnI null mutant, *hdp*^{3}, shows loss of flight and jumping ability, with a drastic hypercontraction phenotype in the IFMs [22,30]. Also, Nongthomba et al. have shown that the IFM-TDT specific TnT null mutant, *up*^{1}, shows loss of only flight and jump ability, and structural defects in IFM and TDT, but normal larval crawling and adult walking ability [25]. Studies conducted on the Drosophila MHC locus have shown that the different, alternatively spliced MHC isoforms, possess differences in their relay or converter domains [64,65], S2 hinge region [66,67] or N-terminus region [68,69]. These different functional domains of the IFM specific MHC isoform, cannot be functionally compensated by the corresponding domains of the embryonic MHC isoforms. These studies show the necessity of expressing the correct isoforms of different myofibrillar proteins in the IFMs for normal physiological function. Our results show that ectopic expression of the short isoform in the IFMs, can weakly compensate for the absence of the long isoform in the IFMs, with regards to flight ability. However, no such functional compensation was seen in the homozygous *Mlp60A*$^{P\text{-}ele}$ mutants, which express a normal short isoform, suggesting that the longer isoform is necessary for normal IFM function. Also, a simultaneous knockdown of both these isoforms leads to an even more severe flight defect and IFM defects. These results collectively show that of the two isoforms being expressed in the IFMs, the long isoform is the major one, governing normal IFM function, and hence, flight ability. In the absence of the long isoform, the short isoform can provide for only a weak flight ability. Hence, a functional specialization exists between the Mlp60A isoforms, such that the short and the long isoform are necessary for the normal development of the larval body wall muscles and the adult IFMs, respectively. A comparison of the rescue of the null mutants with the short isoform versus rescue with the long isoform would have provided additional insight. Towards this end, transgenic lines expressing *Mlp60A-long* under the control of the *UAS* promoter were generated, but these lines completely failed to show any transgenic expression of the long isoform (data not shown). Also, since the antibody specificity couldn't be checked in the null background, we have relied on RT-PCR analysis with at-least two independent long isoform specific primer pairs: *FPShSp-RPLoSp* (Figs. 1D, 6B and 8B) and *FPLoSp-RPLoSp* (Fig. 1E) to study the functional requirement of the long isoform for normal IFM function. A third pair: *FPShIsoCl-RPLoIsoCl*, was used to

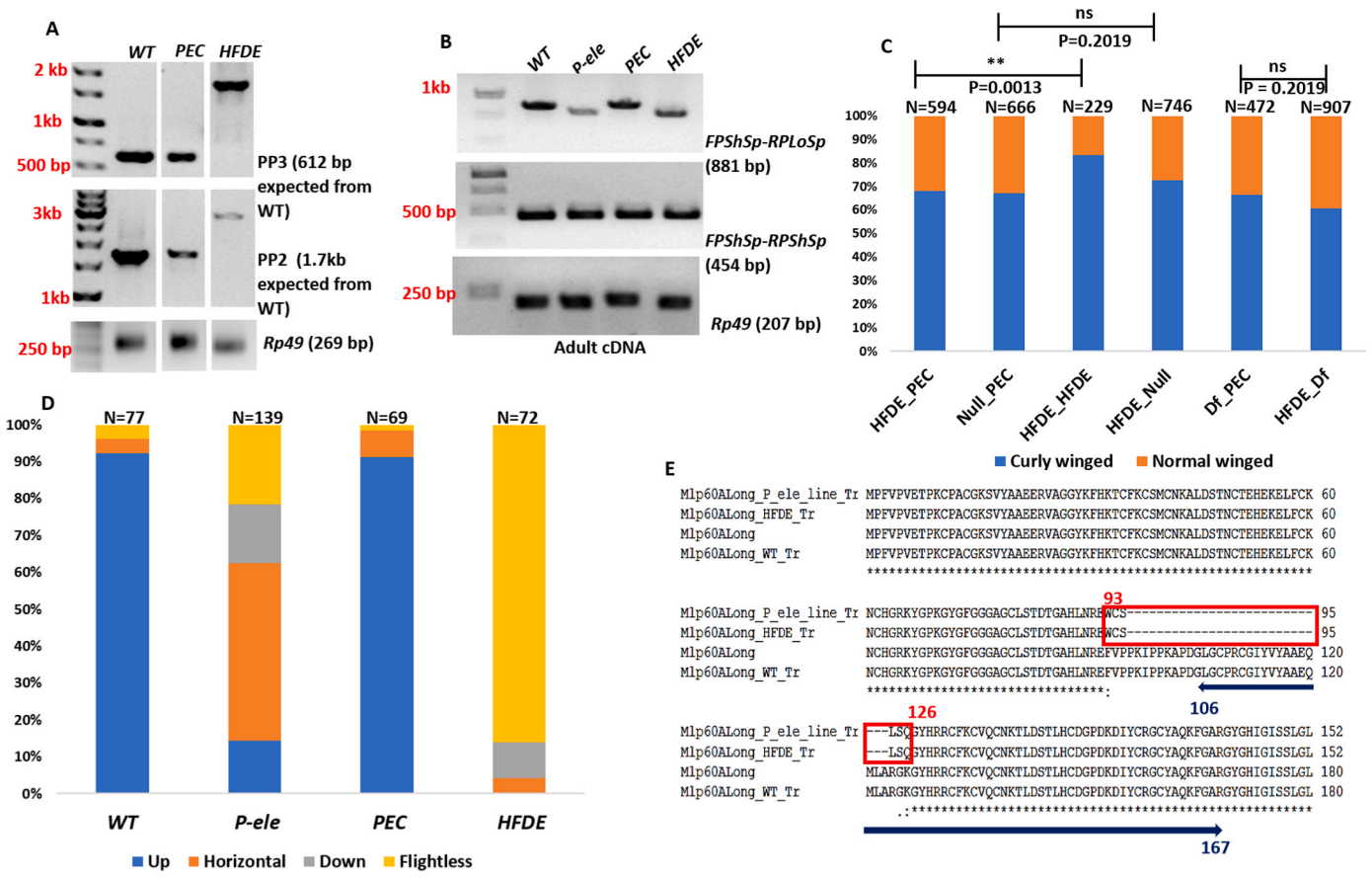

Fig. 8. Phenotypic and molecular characterization of Mlp60A-long isoform-specific alleles-*Mlp60A*$^{P\text{-}ele}$ and *Mlp60A*^{HFDE}. (A) Shows the presence of around 1.3 kb remnant of the original *P-element* insertion, in the *Mlp60A*^{HFDE} allele. *PP3* refers to PCR products of primers FP3 (intron 2–3) and RP3 (exon 5). *PP2* refers to PCR products of primers FP2 (intron 1–2) and RP2 (exon 7). (B) Shows the analysis of *Mlp60A-long* spliced transcript from homozygous *Mlp60A*$^{P\text{-}ele}$ and homozygous *Mlp60A*^{HFDE} mutants. (C) Shows results of complementation tests between the *Mlp60A*^{HFDE} allele and either the *Mlp60A*^{null} allele or a *Mlp60A* genomic deficiency chromosome: *Df(2R)BSC356*. Each bar shows the percentages of curly-winged and normal-winged flies (Y-axis) eclosed in genetic crosses between *CyO-GFP* balanced males/females of respective alleles (X-axis). Homozygous *Mlp60A*^{HFDE} flies survive in a significantly lesser percentage than the *Mlp60A*^{HFDE}*//PEC* flies (CSV = 10.340, df = 1); however, the survival of *Mlp60A*^{HFDE}*//Mlp60A*^{null} flies and *Mlp60A*^{HFDE}*//Df* flies was not significantly different from the respective controls (CSV = 0.2019, df = 1, in both cases) (D) Shows the flight ability of flies of respective genotypes (all homozygotes). Y-axis shows the percentage of flies, and X-axis shows the genotype of normal winged flies, obtained in each cross. (E) Shows the alignment of the translated Mlp60A-long sequences encoded by the *Mlp60A*$^{P\text{-}ele}$, *Mlp60A*^{HFDE} and *wild-type* alleles, along with the database sequence as the reference. The red box shows the sequence of residues of the long isoform, which is different between the wild-type and the mutant long isoform proteins. Residues 93rd to 126th of the wild-type protein are absent from the *Mlp60A*$^{P\text{-}ele}$ and *Mlp60A*^{HFDE} encoded long isoforms. The mutant proteins instead contain a unique sequence of six residues- WCSLSQ. The navy-blue bar labels the sequence of the residues in the wild-type long isoform, which encodes the 2nd LIM domain. Thus, the comparison presented in this figure clearly shows that the *Mlp60A*$^{P\text{-}ele}$ and *Mlp60A*^{HFDE} allele encoded mutant long isoform lacks a part of the 2nd LIM domain.

detect and sequence the full-length long isoform (Fig. 1B and Fig. S1A).

3.3. *The Mlp60A locus is important for normal myofibril assembly in the IFMs*

The IFM phenotype of the *Mlp60A* knockdown flies - frayed myofibrils and formation of actin-rich aggregates-provides *in vivo* evidence that this locus is involved in the regulation of actin dynamics and thin filament assembly, during IFM development. These results corroborate those of a previous study wherein MLP was shown to promote actin crosslinking and bundling of actin filaments, in C2C12 myoblasts [55]. Our results also show that *Mlp60A* knockdown leads to reduced sarcomere length in the IFMs. In a previous study, the knockdown of *Myosin heavy chain (Mhc)* and *Actin 88F (Act88F)* was shown to result in an increased sarcomere length in IFMs, whereas the knockdown of the *bent* (encoding the giant protein-projectin) was shown to result in a decrease in sarcomere length [70]. It is known that shorter sarcomeres lead to the production of significantly lesser force, since it reduces the effective overlap between the actin and myosin filaments, according to the sliding filament principle [71]. We propose that, the IFM knockdown phenotype being very drastic in nature, the reduced sarcomere length could be a compensatory response, to prevent further muscle damage, by reducing the force produced with each contraction cycle. Overall, our knockdown study shows that the *Mlp60A* knockdown flies can serve as a platform for further investigation of MLP function in actin regulation and thin filament assembly during muscle development.

3.4. *Study of Mlp60A alternative splicing and alternate isoform functions can help in understanding the role of CSRP3 in muscle pathophysiology*

In vertebrates, Vafiadaki et al., have reported an alternate isoform of MLP, designated as MLP-b (to differentiate it from the known isoform, renamed MLP-a). This isoform is generated as a result of splicing out of exons 3 and 4 from the primary *CSRP3* transcript [41]. MLP-b levels were upregulated in limb girdle muscular dystrophy (LGMD2A), Duchenne muscular dystrophy (DMD) and Dermatomyositis (DM) patients and the MLP-b/MLP-a ratio was found to be altered in LGMD2A and DMD patients [41]. These results show that the deregulation of MLP

alternative splicing can contribute to the pathogenesis of these diseases. Also, deregulated splicing has been implicated in diseases like Myotonic Dystrophy type 1 (MD1), fascioscapulohumeral dystrophy (FSHD), DCM and HCM [72–78]. Similarly, our results also show the importance of the regulation of *Mlp60A* expression by alternative splicing, because muscle function is compromised when the long isoform is not expressed in the IFMs. Thus, taken together with the previous reports, our results suggest that a future study of the players involved in *Mlp60A* alternative splicing in Drosophila IFMs can greatly aid in understanding the pathogenesis of human muscle diseases in which MLP isoform levels are altered. Also, our results show that losing a part of the 2nd LIM domain of MLP is detrimental to the physiological function (in this case, flight). Even though several *CSRP3* variants have been reported to be linked to HCM disease [35–38,79,80], to this date, only one variant, p.C58G, in the 1st LIM domain of MLP, has been validated to be 'likely pathogenic' [38]. Thus, our results provide additional *in vivo* evidence, pointing towards the possibility that MLP variants may be involved in the development of HCM pathophysiology, which needs further validation.

4. Conclusion

In conclusion, this report sheds light on three significant aspects of MLP function *in vivo*, through the study of the *Mlp60A* locus in *Drosophila melanogaster*. First, the short isoform is necessary for the normal development of larval muscles. Second, the long isoform is necessary for normal IFM function. Third, both these isoforms show functional specialization. Therefore, the short to long isoform switching is necessary for normal physiological flight function. Further studies detailing *Mlp60A* alternative splicing, including the splicing factors, etc., of this locus in *Drosophila melanogaster* could reveal important insights into MLP involvement in human cardiac and skeletal muscle disorders.

5. Materials and Methods

5.1. Fly lines used in the study

The fly lines used in this study were either procured from the Bloomington Drosophila Stock Center (Bloomington University, Indiana) or the Vienna Drosophila Research Center (Vienna BioCenter, Vienna), or were generated in the lab. The following Stocks were used:

(i) *Mlp60A* RNAi line1: BS#29381 (*y* [1] *v* [1]*; P{y[+t7.7] v [+t1.8]=TRiP.JF03313}attP2*).
(ii) *Mlp60A* RNAi line2: VDRC#23511 (*w*^{1118}*; P{GD13576}v23511*).

Fly lines (i) and (ii) were used to achieve the RNAi-mediated knockdown of *Mlp60A* by the *UAS/Gal4* system [43].

(iii) *Drosophila* line containing a source of the genetically engineered *P-element* transposase: "delta 2–3 transposase": BS#4368; (*y* [1] *w* [1]*; Ki* [1] *P{ry[+t7.2]=Delta2-3}99B*).
(iv) *Mlp60A P-element* insertion line: BS#27970; (*y* [1] *w[*]; P{w [+mC]=EP}Mlp60A[G7762]*) [81].

Fly lines (iii) and (iv) were used to perform a hop-out mutagenesis screen, to generate null or isoform-specific *Mlp60A* mutants.

(v) *Dmef2-Gal4* driver line: BS#27390; (*y* [1] *w[*]; P{w[+mC]= GAL4-mef2.R}3*) [82].
(vi) *elav-Gal4* driver line: BS#458; (*P{w[+mW.hs]=GawB}elav [C155]*) [83].
(vii) *UH3-Gal4* driver line: generated in the lab [45].

Fly lines (v-vii) were used as the Gal4 driver lines to achieve tissue-specific knockdown or overexpression of the Mlp60 A.

(vii) A deficiency line of *Mlp60A* region: BS#24380; (*w1118; Df(2R) BSC356/SM6a*).

Apart from these lines, the various balancer chromosomes, wherever required, were used as per the standard methodology of genetic crosses for *Drosophila melanogaster* [84].

5.2. Maintenance and culturing of flies

The flies were cultured using the standard *Drosophila* medium (Cornmeal-Agar-Sucrose-yeast) at 25 °C. Crosses for tissue-specific knockdown or over-expression using the *Gal4/UAS* system were carried out at 29 °C. The larvae, wherever required, were collected and reared on a larval collection medium with the following composition: 2.5% ethanol, 1.5% Glacial Acetic Acid, 1.5% agar, 2.5% sucrose; with a thick yeast paste as the major food source.

5.3. Genetic complementation tests and rescue

The complementation tests were carried out by crossing together the *CyO-GFP* balanced fly stocks of the respective alleles (or the deficiency chromosome). The percentages of *trans*-heterozygous (normal winged) and curly winged flies obtained in the resulting progeny were compared with those obtained in the respective control cross, in which one of the test stocks was crossed to the *PEC//CyO-GFP* fly stock, to yield normal winged and curly winged flies according to Mendelian ratios.

The rescue experiment was performed using a similar strategy. The flies of *Mlp60A*^{null}*//CyO-GFP; UAS-Mlp60A-short* genotype were crossed with flies of either genotypes: *Mlp60A*^{null}*//CyO-GFP* (negative control set), or *PEC//CyO-GFP* (positive control set), or *UH3-Gal4; Mlp60A*^{null}*// CyO-GFP* (test set). The percentages of normal and curly winged flies obtained in each set were then compared to assess the extent of rescue.

5.4. Genetic crosses to generate P-element hop outs

Through the appropriate genetic crosses, the *P-element* insertion bearing chromosome and the chromosome carrying the transposase gene were brought together. Flies of this genotype were mated with flies carrying the 2nd chromosome balancer: *Tft//CyO-GFP*. From the progeny, each white eyed male fly (hop out) was mated with *Tft//CyO-GFP* virgin flies in a separate vial, to obtain stable lines. The progenies from such crosses (stable lines) were then subjected to 'selfing' and screened for phenotypes.

5.5. Flight test

Flies were tested for their flight ability using the 'Sparrow box' method as described previously [61]. Each fly was tested 2–3 times and results were presented as percentages of flies showing each type of flight ability- Up, Horizontal, Down or Flightless, as per their flight in the Sparrow box. All flight tests were performed with 3–5 day old flies.

5.6. Test of larval locomotion

Third instar larvae were tested for their crawling ability on a 1% agar plate. The animals were transferred onto a moist 1% agar plate (90 mm dish) and allowed to acclimatize for about 30s. Following this, they were allowed to crawl for 42s, during which time videos were captured using a digital camera (8 Mega Pixel). The recorded videos were then analysed using the "MtrackJ" plugin with ImageJ v1.52k (https://imagej.nih.gov/ij/).

5.7. Visualization of IFMs through polarized light microscopy

The fly hemi-thoraces were processed for visualization of IFM fascicular structure by polarized light microscopy as described

previously [85,86]. Following preparation, the hemi-thoraces were observed using an Olympus SZX12 microscope with a polarizer and analyser attachment. Images were captured using a Leica DFC300 FX camera. The age of the flies dissected and visualized was 3–5 days old.

5.8. Dissection and visualization of larval body wall muscles by confocal microscopy

Third instar larvae were immobilized by placing them on ice in a cavity block for 30 min. These were then dissected by placing them in 1X PBS on a Silguard plate. Following this, the larvae were fixed by using 70% alcohol for 30 min washed with 1X PBS, 3 times, on a rocker and then stained with 1:40 diluted Phalloidin-TRITC (Sigma) for a period of 1 h at room temperature. Then the larvae were washed again using 1X PBS and then mounted on a slide using 1:1 mixture of Glycerol and Vectashield (https://vectorlabs.com/vectashield-mounting-medium.html) as the mounting agent. The cover slips were then sealed with transparent nail paint and then stored at 4 °C. These samples were then visualized under a confocal microscope (either Zeiss LSM 510 META or Leica SP8 confocal imaging system).

5.9. Visualization of IFM structure by immunostaining and confocal microscopy

Dissections and sample preparation for confocal microscopy to visualize the transverse (cross) sections and longitudinal sections of IFMs were performed as described previously [87]. The Z-discs were marked in the longitudinal sections by using mouse anti α-actinin primary antibody (DSHB Hybridoma, Product 47-18-9). The muscle membrane was marked using mouse anti β-*PS*-Integrin primary antibody (DSHB Hybridoma, Product CF.6G11). Both these primary antibodies were used with 1:100 dilution. The secondary antibody used in both cases was anti-mouse AL488 (Invitrogen), at 1:250 dilution. The anti-Mlp60A antibody, generated in the lab to study Mlp60A localization, was used with 1:1000 dilution. Samples were visualized using either Zeiss LSM 510 META or Leica SP8 confocal imaging system. The age of the flies dissected and visualized was 3–5 days old.

5.10. Assessment of developmental lethality

To assess the effective lethal stage of mutants, eggs were collected on a 2.5% sucrose, 1.5% agar medium in 60 mm petri plates. Following the collection of eggs, they were allowed to hatch and the L1 larvae were transferred to an egg collection medium with an additional 1.5% glacial acetic acid and 2.5% ethanol. Then their development was monitored to check up to which stage each individual survived. The lethality was calculated as per the percentage of total fertilized eggs or L1 larvae initially collected, that died in the subsequent larval or pupal developmental stages [88].

5.11. Genomic DNA isolation

Genomic DNA was isolated from either whole flies or whole larvae using the Qiagen' DNeasy Blood and Tissue' DNA isolation kit (Catalogue no:69,504). The isolated genomic DNA was quantified by using NANODROP 1000 or NANODROP Lite spectrophotometers by ThermoFisher Scientific.

5.12. RNA isolation and cDNA preparation

Either whole animals (adults, L1 larvae, L3 larvae or pupae of different stages) or tissues (adult head, thorax or abdomen or IFMs) were collected for RNA isolation using the TRI reagent (Sigma) based protocol. The isolated RNA was quantified by using NANODROP 1000 or NANODROP Lite Spectrophotometers by ThermoFisher Scientific. The integrity of the isolated RNA was assessed by running 1 μL of isolated RNA on 1% agarose gel. Reverse transcription reaction was carried out using the first-strand cDNA synthesis kit by ThermoFisher Scientific.

5.13. Qualitative polymerase chain reactions

PCRs were carried out using 2X PCR Master mix (Taq Polymerase) by ThermoFisher Scientific (Catalogue No: K1072). High fidelity PCRs, wherever required, were carried out by using ThermoFisher Scientific Phusion DNA polymerase (Catalogue No: F530S). The products resulting from PCR were resolved on agarose gels of different compositions (0.8%, 1% or 2%) and imaged.

5.14. Quantitative polymerase chain reactions

qRT-PCRs were carried out to assess relative gene expression in different samples. The reactions and data analyses were carried according to the 'delta (delta) Ct' method as described by Livak and Schmittgen, 2001 [89]. In cases, wherever required, only delta C_t was plotted. The reactions were carried out using the 'SYBR Green Master Mix' by Bio-Rad or the 'DyNamo SYBR Green qPCR kit' by ThermoFisher Scientific (Catalogue No: F-410L).

5.15. Sequencing of DNA fragments

DNA fragments amplified by PCR and sequenced, either after performing a clean-up with 'QIA Quick PCR Purification Kit' (QIAGEN Catalog No: 28,104), or after generating clones through TA cloning (TA-cloned using the 'ThermoFisher Scientific InsTAclone PCR Cloning Kit', Catalogue No: K1214). Samples were sequenced at AgriGenome Labs.

5.16. Generation of transgenic UAS lines for conditional expression of Mlp60 A-short isoform

The *Mlp60A-short* specific CDS was cloned within the *pUASt-attB* vector following the usual methodology for restriction digestion-based cloning. The *pUASt-attB-Mlp60A-short* plasmid construct was submitted to 'Fly Facility, NCBS' (http://www.ccamp.res.in/Fly-facility), for microinjection into embryos carrying *attP2* docking site on the 3rd chromosome for *attP2-attB* mediated site-specific insertion of the constructs. The microinjection and screening for transgenics were performed by the Fly Facility. Two transgenic lines were obtained, one of which was used for the experiments.

5.17. Molecular cloning

DNA fragments were cloned by restriction digestion-ligation based procedure, for which all enzymes were obtained from ThermoFisher Scientific. *E. coli* DH5α competent cells were prepared by the TSS protocol [90]. The transformation was done using the heat-shock protocol [91]. The colonies were screened by PCR with insert-specific primers, following which plasmids were isolated using the 'GSURE Plasmid Mini' kit by GCC Biotech (Catalogue No: G4613).

5.18. Raising polyclonal antibody against Mlp60 A short isoform

The polyclonal antibody was raised against the short Mlp60A isoform of 10 kDa size by cloning the transcript into the pET15b protein expression vector after confirming the sequence (Macrogen, South Korea) for any mutation. Then, the protein was expressed in the *E. coli* BL21 (DE3) endo strain, upon induction using 0.4 mM isopropyl B-D-1-thiogalactopyranoside (IPTG) for 6 h at 25 °C and injecting the expressed product into a rabbit to raise antibody.

5.19. Protein extraction and Western blot

IFMs were dissected from bisected flies preserved in 70% alcohol and

homogenized in 1x Buffer (0.1 M NaCl, 10 mM potassium phosphate pH 7.0, 2 mM EGTA, 2 mM $MgCl_2$, 1 mM DTT, 1 mM PMSF and 0.5% Triton-X). The IFM lysate was spun down to obtain a protein pellet which was further washed with the same 1X buffer but without Triton-X and then boiled in SDS-sample buffer (0.0625 M Tris-Cl pH 6.8, 2% SDS,10% glycerol, 5% 2-mercaptoethanol and 5 μg bromophenol blue) for 4 min at 95 °C. Samples were then resolved in a 12% PAGE gel in a mini electrophoresis unit (Amersham) at 100 V. The protein was then transferred from the gel to a PVDF membrane (Immobilon-P, Millipore) in transfer buffer (20% methanol, 25 mM Tris-base and 150 mM glycine). The membrane was blocked with 8% milk solution in Tris buffer saline (TBS, pH 7.4) for 1 h and then probed with the Anti-Mlp60A antibody (1:1000 dilution) overnight at 4 °C. After washing three times with TBS, the membrane was incubated with the HRP-conjugated secondary antibody (anti-rabbit 1:1000, Bangalore Genei, Bangalore) for 3 h at room temperature. The membrane was then washed three times (15 min each) with TBST (TBS with 0.05% Tween 20) and 5 min with 0.5 M NaCl. Bands were detected by using the enhanced chemiluminescence (ECL) method (Supersignal WestPico Chemiluminescent substrate, Pierce).

5.20. Primers used in this study

Supplementary Table S1 lists the primers that were used in this study, along with the purpose for which each was used.

5.21. Quantifications and statistical analyses

Phenotypic parameters were quantified using ImageJ v1.52k (for IFM fascicular width, total fascicular area and sarcomere length quantification) or the LSM Image browser (for larval body wall muscle width measurement). The resulting data were plotted in GraphPad Prism v5.00 and the statistical significance was determined by using an unpaired Student's t-test. Statistical significance for qPCR data was carried out using paired Student's t-test. The chi-squared test was carried out to determine statistical significance in data sets with categorical data.

Credit author statement

- MJ along with SRR and UN conceived and performed the experiments pertaining to Mlp60A polyclonal antibody generation and the associated Western blotting and Immunostaining.
- RW and UN conceived and planned all the other experiments being reported in the manuscript, and these were performed exclusively by RW.
- Paper was written by RW and UN and approved by all the authors before submission.

Declaration of competing interest

Authors declare that there is NO conflicts of interest and funders had no influence in experimental design and data collection or outcome. We confirm that the manuscript has been read and approved by all named authors.

Data availability

Data will be made available on request.

Acknowledgements

We thank the Bioimaging facility and Animal facility at the Indian Institute of Science (IISc) for their aid. We also thank the University Grants Commission, Ministry of Human Resource Development (MHRD), Govt. Of India, for research fellowship (Sr No: 2121330889, Ref No: December 22, 2013(ii)EU-V). This worked was supported by SERB, Department of Science and Technology (DST), Govt. Of India, grant (EMR/2016/004563) to UN. We also acknowledge the Indian Institute of Science (IISc), the Department of Science and Technology (DST), Govt. Of India, (DST FIST, Ref. No. SR/FST/LSII-036/2014), the University Grant Commission (UGC-SAP to MRDG: Ref. No. F.4-13/2018/DRS-III (SAP-II) and the Department of Biotechnology (DBT), Govt. Of India, (DBT-IISC Partnership Program Phase-II (BT/PR27952-INF/22/212/2018) for infrastructure and financial assistance. We also would like to acknowledge anonymous reviewers and Mr. Amartya Mukherjee, for their insightful comments and suggestions which allowed us to improve the manuscript.

Appendix A. Supplementary data

Supplementary data to this article can be found online at https://doi.org/10.1016/j.yexcr.2022.113430.

References

[1] E. Bandman, Contractile protein isoforms in muscle development, Dev. Biol. 154 (1992) 273–283.
[2] T.S. Wong, C.P. Ordahl, Troponin T gene switching is developmentally regulated by plasma-borne factors in parabiotic chicks, Dev. Biol. 180 (1996) 732–744.
[3] D. Pette, R.S. Staron, Myosin isoforms, muscle fiber types, and transitions, Microsc. Res. Tech. 50 (2000) 500–509.
[4] R.Y.C.R. Bottinelli, C. Reggiani, Human skeletal muscle fibres: molecular and functional diversity, Prog. Biophys. Mol. Biol. 73 (2000) 195–262.
[5] Y. Mizuno, M. Suzuki, H. Nakagawa, N. Ninagawa, S. Torihashi, Switching of actin isoforms in skeletal muscle differentiation using mouse ES cells, Histochem. Cell Biol. 132 (2009) 669.
[6] A.E. Brinegar, et al., Extensive alternative splicing transitions during postnatal skeletal muscle development are required for calcium handling functions, Elife 6 (2017), 27192.
[7] M. Savarese, et al., The complexity of titin splicing pattern in human adult skeletal muscles, Skeletal Muscle 8 (2018) 11.
[8] M.L. Spletter, F. Schnorrer, Transcriptional regulation and alternative splicing cooperate in muscle fiber-type specification in flies and mammals, Exp. Cell Res. 321 (2014) 90–98.
[9] B.E. Swyngedouw, Developmental and functional adaptation of contractile proteins in cardiac and skeletal muscles, Physiol. Rev. 66 (1986) 710–771.
[10] R.N. Kitsis, A.J. Scheuer, Functional significance of alterations in cardiac contractile protein isoforms, Clin. Cardiol. 19 (1996) 9–18.
[11] M.B. Chechenova, et al., Functional redundancy and non-redundancy between two Troponin C isoforms in Drosophila adult muscles, Mol. Biol. Cell 28 (2017) 760–770.
[12] S. Schiaffino, C. Reggiani, Fiber types in mammalian skeletal muscles, Physiol. Rev. 91 (2011) 1447–1531.
[13] M.V. Taylor, Comparison of muscle development in Drosophila and vertebrates, in: Muscle Development in Drosophila vols. 169–203, Springer, New York, NY, 2006.
[14] M. Rai, U. Nongthomba, M.D. Grounds, Skeletal muscle degeneration and regeneration in mice and flies, Curr. Top. Dev. Biol. 108 (2014) 247–281.
[15] J.W.S. Pringle, The Croonian Lecture, 1977-Stretch activation of muscle: function and mechanism, Philos. Trans. R. Soc. Lond. B Biol. 201 (1978) 107–130.
[16] M. Peckham, J.E. Molloy, J.C. Sparrow, D.C.S. White, Physiological properties of the dorsal longitudinal flight muscle and the tergal depressor of the trochanter muscle of Drosophila melanogaster, J. Muscle Res. Cell Motil. 11 (1990) 203–215.
[17] C. Schönbauer, et al., Spalt mediates an evolutionarily conserved switch to fibrillar muscle fate in insects, Nature 479 (2011) 406–409.
[18] E.A. Fyrberg, J.W. Mahaffey, B.J. Bond, N. Davidson, Transcripts of the six Drosophila actin genes accumulate in a stage-and tissue-specific manner, Cell 33 (1983) 115–123.
[19] S. Falkenthal, M. Graham, J. Wilkinson, The indirect flight muscle of Drosophila accumulates a unique myosin alkali light chain isoform, Dev. Biol. 121 (1987) 263–272.
[20] G.A. Hastings, C.P. Emerson, Myosin functional domains encoded by alternative exons are expressed in specific thoracic muscles of Drosophila, J. Cell Biol. 114 (1991) 263–276.
[21] Q.I.U. Feng, et al., Troponin C in different insect muscle types: identification of two isoforms in Lethocerus, Drosophila and Anopheles that are specific to asynchronous flight muscle in the adult insect, Biochem. J. 371 (2003) 811–821.
[22] J.A. Barbas, J. Galceran, L. Torroja, A. Prado, A. Ferrus, Abnormal muscle development in the heldup3 mutant of Drosophila melanogaster is caused by a splicing defect affecting selected troponin I isoforms, Mol. Cell Biol. 13 (1993) 1433–1439.
[23] J.O. Vigoreaux, J.D. Saide, K. Valgeirsdottir, M.L. Pardue, Flightin, a novel myofibrillar protein of Drosophila stretch-activated muscles, J. Cell Biol. 121 (1993) 587–598.
[24] C. Burkart, et al., Modular proteins from the Drosophila sallimus (sls) gene and their expression in muscles with different extensibility, J. Mol. Biol. 367 (2007) 953–969.

[25] U. Nongthomba, M. Ansari, D. Thimmaiya, M. Stark, J. Sparrow, Aberrant splicing of an alternative exon in the Drosophila troponin-T gene affects flight muscle development, Genetics 177 (2007) 295–306.
[26] Z. Orfanos, J.C. Sparrow, Myosin isoform switching during assembly of the Drosophila flight muscle thick filament lattice, J. Cell Sci. 126 (2013) 139–148.
[27] P.T. O'Donnell, V.L. Collier, K. Mogami, S.I. Bernstein, Ultrastructural and molecular analyses of homozygous-viable Drosophila melanogaster muscle mutants indicate there is a complex pattern of myosin heavy-chain isoform distribution, Genes Dev. 3 (1989) 1233–1246.
[28] P. Benoist, J.A. Mas, R. Marco, M. Cervera, Differential muscle-type expression of the Drosophila troponin T gene- A 3-base pair microexon is involved in visceral and adult hypodermic muscle specification, J. Biol. Chem. 273 (1998) 7538–7546.
[29] U. Nongthomba, S. Pasalodos-Sanchez, S. Clark, J.D. Clayton, J.C. Sparrow, Expression and function of the Drosophila ACT88F actin isoform is not restricted to the indirect flight muscles, J. Muscle Res. Cell Motil. 22 (2001) 111–119.
[30] U. Nongthomba, S. Clark, M. Cummins, M. Ansari, M. Stark, J.C. Sparrow, Troponin I is required for myofibrillogenesis and sarcomere formation in Drosophila flight muscle, J. Cell Sci. 117 (2004) 1795–1805.
[31] S. Arber, G. Halder, P. Caroni, Muscle LIM protein, a novel essential regulator of myogenesis, promotes myogenic differentiation, Cell 79 (1994) 221–231.
[32] Y. Kong, M.J. Flick, A.J. Kudla, S.F. Konieczny, Muscle LIM protein promotes myogenesis by enhancing the activity of MyoD, Mol. Cell Biol. 17 (1997) 4750–4760.
[33] S. Arber, et al., MLP-deficient mice exhibit a disruption of cardiac cytoarchitectural organization, dilated cardiomyopathy, and heart failure, Cell 88 (1997) 393–403.
[34] B.J. Maron, et al., American College of Cardiology/European Society of Cardiology clinical expert consensus document on hypertrophic cardiomyopathy: a report of the American College of Cardiology foundation task force on clinical expert consensus documents and the European Society of Cardiology committee for practice guidelines, J. Am. Coll. Cardiol. 42 (2003) 1687–1713.
[35] C. Geier, et al., Beyond the sarcomere: CSRP3 mutations cause hypertrophic cardiomyopathy, Hum. Mol. Genet. 17 (2008) 2753–2765.
[36] R.E. Hershberger, et al., Genetic evaluation of cardiomyopathy—a Heart Failure Society of America practice guideline, J. Card. Fail. 15 (2009) 83–97.
[37] A. Janin, F. Bessière, S. Chauveau, P. Chevalier, G. Millat, First identification of homozygous truncating CSRP3 variants in two unrelated cases with hypertrophic cardiomyopathy, Gene 676 (2018) 110–116.
[38] M. Ehsan, et al., Mutant Muscle LIM Protein C58G causes cardiomyopathy through protein depletion, J. Mol. Cell. Cardiol. 121 (2018) 287–296.
[39] I.A. Barash, L. Mathew, M. Lahey, M.L. Greaser, R.L. Lieber, Muscle LIM protein plays both structural and functional roles in skeletal muscle, Am. J. Physiol. Cell Physiol. 289 (2005) C1312–C1320.
[40] Y. Chang, F. Geng, Y. Hu, Y. Ding, R. Zhang, Zebrafish cysteine and glycine-rich protein 3 is essential for mechanical stability in skeletal muscles, Biochem. Biophys. Res. Commun. 511 (2019) 604–611.
[41] E. Vafiadaki, et al., Muscle LIM protein isoform negatively regulates striated muscle actin dynamics and differentiation, FEBS J. 281 (2014) 13261–13279.
[42] B.E. Stronach, S.E. Siegrist, M.C. Beckerle, Two muscle-specific LIM proteins in Drosophila, J. Cell Biol. 134 (1996) 1179–1195.
[43] A.H. Brand, N. Perrimon, Targeted gene expression as a means of altering cell fates and generating dominant phenotypes, Development 118 (1993) 401–415.
[44] K. O'Hare, G.M. Rubin, Structures of P transposable elements and their sites of insertion and excision in the Drosophila melanogaster genome, Cell 34 (1983) 25–35.
[45] S.H. Singh, P. Kumar, N.B. Ramachandra, U. Nongthomba, Roles of the troponin isoforms during indirect flight muscle development in Drosophila, J. Genet. 93 (2014) 379–388.
[46] K. Mogami, Y. Hotta, Isolation of Drosophila flightless mutants which affect myofibrillar proteins of indirect flight muscle, Mol. Gen. Genet. 183 (1981) 409–417.
[47] C.J. Beall, M.A. Sepanski, E.A. Fyrberg, Genetic dissection of Drosophila myofibril formation: effects of actin and myosin heavy chain null alleles, Genes Dev. 3 (1989) 131–140.
[49] S. Arber, P. Caroni, Specificity of single LIM motifs in targeting and LIM/LIM interactions in situ, Genes Dev. 10 (1996) 289–300.
[50] H. Holtzer, J.M. Marshall, H. Finck, An analysis of myogenesis by the use of fluorescent antimyosin, J. Cell Biol. 3 (1957) 705–724.
[51] S.M. Abmayr, M.S. Erickson, B.A. Bour, Embryonic development of the larval body wall musculature of Drosophila melanogaster, Trends Genet. 11 (1995) 153–159.
[52] F. Demontis, N. Perrimon, Integration of Insulin receptor/Foxo signaling and dMyc activity during muscle growth regulates body size in Drosophila, Development 136 (2009) 983–993.
[53] A. Chesley, J.D. MacDougall, M.A. Tarnopolsky, S.A. Atkinson, K. Smith, Changes in human muscle protein synthesis after resistance exercise, J. Appl. Physiol. 73 (1992) 1383–1388.
[54] V. Papalouka, et al., Muscle LIM protein interacts with cofilin 2 and regulates F-actin dynamics in cardiac and skeletal muscle, Mol. Cell Biol. 29 (2009) 6046–6058.
[55] C. Hoffmann, et al., Human muscle LIM protein dimerizes along the actin cytoskeleton and cross-links actin filaments, Mol. Cell Biol. 34 (2014) 3053–3065.
[56] M.M. Rashid, et al., Muscle LIM protein/CSRP3: a mechanosensor with a role in autophagy, Cell Death Dis. 1 (2015) 1–12.
[57] Y. Yan, H. Wang, H. Chen, A. Lindström-Battle, R. Jiao, Ecdysone and insulin signaling play essential roles in readjusting the altered body size caused by the dGPAT4 mutation in Drosophila, J. Genet. Genomics 42 (2015) 487–494.
[58] K.A. Clark, J.M. Bland, M.C. Beckerle, The Drosophila muscle LIM protein, Mlp84B, cooperates with D-titin to maintain muscle structural integrity, J. Cell Sci. 120 (2007) 2066–2077.
[59] D.M. Swank, et al., Alternative exon-encoded regions of Drosophila myosin heavy chain modulate ATPase rates and actin sliding velocity, J. Biol. Chem. 276 (2001) 15117–15124.
[60] S. Zhang, S.I. Bernstein, Spatially and temporally regulated expression of myosin heavy chain alternative exons during Drosophila embryogenesis, Mech. Dev. 101 (2001) 35–45.
[61] D.R. Drummond, E.S. Hennessey, J.C. Sparrow, Characterisation of missense mutations in the Act88F gene of Drosophila melanogaster, Mol. Gen. Genet. 226 (1991) 70–80.
[62] H. An, K. Mogami, Isolation of 88F Actin mutants of Drosophila melanogaster and possible alterations in the mutant actin structures, J. Mol. Biol. 260 (1996) 492–505.
[63] T.E. Dohn, R.M. Cripps, Absence of the Drosophila jump muscle actin Act79B is compensated by up-regulation of Act88F, Dev. Dynam. 247 (2018) 642–649.
[64] W.A. Kronert, C.M. Dambacher, A.F. Knowles, D.M. Swank, S.I. Bernstein, Alternative relay domains of Drosophila melanogaster myosin differentially affect ATPase activity, in vitro motility, myofibril structure and muscle function, J. Mol. Biol. 379 (2008) 443–456.
[65] W.A. Kronert, G.C. Melkani, A. Melkani, S.I. Bernstein, Alternative relay and converter domains tune native muscle myosin isoform function in Drosophila, J. Mol. Biol. 416 (2012) 543–557.
[66] J.A. Suggs, et al., Alternative S2 hinge regions of the myosin rod differentially affect muscle function, myofibril dimensions and myosin tail length, J. Mol. Biol. 367 (2007) 1312–1329.
[67] M.S. Miller, et al., Alternative S2 hinge regions of the myosin rod affect myofibrillar structure and myosin kinetics, Biophys. J. 96 (2009) 4132–4143.
[68] D.M. Swank, W.A. Kronert, S.I. Bernstein, D.W. Maughan, Alternative N-terminal regions of Drosophila myosin heavy chain tune muscle kinetics for optimal power output, Biophys. J. 87 (2004) 1805–1814.
[69] D.M. Swank, et al., An alternative domain near the ATP binding pocket of Drosophila myosin affects muscle fiber kinetics, Biophys. J. 90 (2006) 2427–2435.
[70] A.D. Perkins, G. Tanentzapf, An ongoing role for structural sarcomeric components in maintaining Drosophila melanogaster muscle function and structure, PLoS One 9 (2014), e99362.
[71] D.E. Rassier, B.R. MacIntosh, W. Herzog, Length dependence of active force production in skeletal muscle, J. Appl. Physiol. 86 (1999) 1445–1457.
[72] R. Tupler, G. Perini, M.A. Pellegrino, M.R. Green, Profound misregulation of muscle-specific gene expression in facioscapulohumeral muscular dystrophy, Proc. Natl. Acad. Sci. USA 96 (1999) 12650–12654.
[73] S.F. Nagueh, et al., Altered titin expression, myocardial stiffness, and left ventricular function in patients with dilated cardiomyopathy, Circulation 110 (2004) 155–162.
[74] M. Pistoni, C. Ghigna, D. Gabellini, Alternative splicing and muscular dystrophy, RNA Biol. 7 (2010) 441–452.
[75] T.H. Ho, et al., Muscleblind proteins regulate alternative splicing, EMBO J. 23 (2004) 3103, 3012.
[76] J.D. Brook, et al., Molecular basis of myotonic dystrophy: expansion of a trinucleotide (CTG) repeat at the 3′ end of a transcript encoding a protein kinase family member, Cell 68 (1992) 799–808.
[77] J.W. Miller, et al., Recruitment of human muscleblind proteins to (CUG) n expansions associated with myotonic dystrophy, EMBO J. 19 (2000) 4439–4448.
[78] R.N. Kanadia, et al., A muscleblind knockout model for myotonic dystrophy, Science 302 (2003) 1978–1980.
[79] C. Geier, et al., Mutations in the human muscle LIM protein gene in families with hypertrophic cardiomyopathy, Circulation 107 (2003) 1390–1395.
[80] R. Knöll, et al., A common MLP (muscle LIM protein) variant is associated with cardiomyopathy, Circ. Res. 106 (2010) 695–704.
[81] H.J. Bellen, et al., The Drosophila gene disruption project: progress using transposons with distinctive site specificities, Genetics 188 (2011) 731–743.
[82] F. Schnorrer, et al., Systematic genetic analysis of muscle morphogenesis and function in Drosophila, Nature 464 (2010) 287–291.
[83] D.M. Lin, C.S. Goodman, Ectopic and increased expression of Fasciclin II alters motoneuron growth cone guidance, Neuron 13 (1994) 507–523.
[84] R.J. Greenspan, Fly Pushing: the Theory and Practice of Drosophila Genetics, CSHL Press, 2004.
[85] U. Nongthomba, N.B. Ramachandra, A direct screen identifies new flight muscle mutants on the Drosophila second chromosome, Genetics 153 (1999) 261–274.
[86] S.S. Salvi, R.P. Kumar, N.B. Ramachandra, J.C. Sparrow, U. Nongthomba, Mutations in Drosophila myosin rod cause defects in myofibril assembly, J. Mol. Biol. 419 (2012) 22–40.
[87] M. Rai, U. Nongthomba, Effect of myonuclear number and mitochondrial fusion on Drosophila indirect flight muscle organization and size, Exp. Cell Res. 319 (2013) 2566–2577.
[88] M. Ashburner, Drosophila: A Laboratory Handbook, Cold spring harbor laboratory press, 1989.
[89] K.J. Livak, T.D. Schmittgen, Analysis of relative gene expression data using real-time quantitative PCR and the 2− ΔΔCT method, Methods 25 (2001) 402–408.
[90] C.T. Chung, S.L. Niemela, R.H. Miller, One-step preparation of competent Escherichia coli: transformation and storage of bacterial cells in the same solution, Proc. Natl. Acad. Sci. USA 86 (1989) 2172–2175.
[91] A. Froger, J.E. Hall, Transformation of plasmid DNA into E. coli using the heat shock method, JoVE 6 (2007) 253.